

# High surface area TiO<sub>2</sub> photocatalyst for H<sub>2</sub> production through silicon micromachining

Maria Isabel MENDOZA DIAZ

LAAS-CNRS, University of Toulouse, 7 Avenue du colonel Roche, 31400 Toulouse, France

A new concept for a 3D microstructured photocatalyst for hydrogen production by water-splitting under direct sunlight is proposed. The optimization process of deep-reactive ion etching process and the subsequent deposition of TiO<sub>2</sub> thin films by physical vapor deposition decorated with Au nanoparticles allows H<sub>2</sub> production by direct water splitting. The influence of the area enlargement factor on the 3D photocatalyst surface morphology and its photocatalytic performance under UV-visible irradiation was thoroughly analyzed and corroborated by electrochemical experiments. The photocatalyst exhibited an increase in H<sub>2</sub> production by almost a factor of 12 compared to conventional planar TiO<sub>2</sub> films.

## I. INTRODUCTION

An attractive approach for the energy industry's transition to sustainable and clean energy is the use of solar radiation to produce hydrogen.<sup>1</sup> Among the different artificial photocatalytic processes, H<sub>2</sub> production through water splitting (WS) is probably the most intensely studied since H<sub>2</sub> exhibits a high volumetric energy density and no carbon footprint.<sup>2</sup> Among a large choice of proposed photocatalysts TiO<sub>2</sub> remains the most suitable catalyst due to its performance, easy accessibility, nontoxicity and low price.<sup>3</sup> A good strategy to improve the hydrogen production rate is to augment the surface-to-volume ratio by creating high surface microstructures.<sup>4,5</sup> The present study proposes silicon micromachining to fabricate well-defined three-dimensional (3D) geometries of TiO<sub>2</sub> photocatalysts. Next, the influence of the area enlargement factor (AEF) on the morphology, quality and catalytic performance of the 3D photocatalyst was thoroughly investigated. We show that the H<sub>2</sub> production rate can be improved ten times compared to a

planar topology. Moreover, H<sub>2</sub> production is improved by a factor of four through the growth of Au nanoparticles inside the continuous TiO<sub>2</sub> catalytic layer<sup>6</sup>, leading to a UV/visible synergistic effect.<sup>7,8</sup>

## II. MATERIALS AND METHODS

The technological process starts with a silicon substrate: i) photolithography process, positive photoresist (PR; AZ-40XT, MicroChemicals, 20 μm); ii) silicon etching by DRIE Bosch process (AMS420 reactor, Alcatel-Adixen); iii) thermic oxidation and oxide removal with HF; iv) TiO<sub>2</sub> sputtered by direct current magnetron.

Scanning electronic microscopy (SEM, FEI Helios 600i Nanolab), grazing incidence X-ray diffraction (GI-XRD, Bruker D8 Discover system), X-ray photoelectron spectroscopy (XPS, ESCALAB 250 X-ray photoelectron spectrometer) and UV/Vis absorption spectroscopy (Perkin-Elmer Lambda 650 Spectrometer). For photocatalytic experiments,

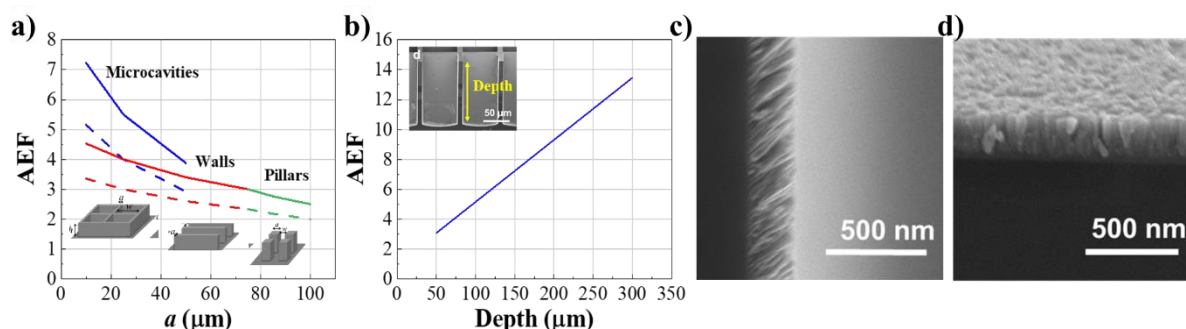


**Figure 1.** (a) Impact of cavity separation on AEF for different patterns. (b) Impact of depth on the AEF for the square microcavity. SEM cross-sectional images of the 3D photocatalyst (depth 150 μm) (b) inset, Si/ TiO<sub>2</sub> interface at (c) half-heights of the wall (d) bottom of the microcavities.

the samples were placed into a quartz reactor (60 mL) with an aqueous solution (10 mL, 35% v/v ethanol) and connected to a gas chromatography apparatus (GC, Perkin-Elmer Clarus 580). Xenon light lamp irradiation (Cemax® PE300B-10F). Electrochemical measurements carried out in a three-electrode configuration (VMP-3, Biologic potentiostat). Cyclic voltammetry performed at 30 mV/s in 0.5 M H<sub>2</sub>SO<sub>4</sub>.

### III. RESULTS AND DISCUSSION

#### A. Si microstructure design

In this work three patterns were studied for the microstructures: square microcavities, walls, and pillars (**Figure 1a**). Each pattern is characterized by the Area Enlargement Factor (AEF) which is calculated from the 3D total surface area divided by the flat area. The *a* parameter is set as the spacing in the patterns. Also, the aspect ratio plays an important role: for magnetron sputtering an aspect ratio  $\leq 2$  is necessary in order to ensure a continuous film deposition. **Figure 1a** shows microcavities as the best pattern to reach a higher AEF. Furthermore, the AEF can be tuned by increasing the depth of the microcavities as shown in **Figure 1b**.

Technical control over the profile and *depth* is achieved by tuning the ratio of the exposure times of SF<sub>6</sub> to C<sub>4</sub>F<sub>8</sub>/O<sub>2</sub> gases; and the total time of the DRIE process. SEM observations

(**Figure 1b** inset) show the microcavities with a smooth surface and very defined vertical walls.

#### A. 3D photocatalysts characterization

To study the impact of the enlarged surfaces on the H<sub>2</sub> production rate, silicon microstructures were fabricated with defined AEFs of 3, 5 and 7, which correspond to microcavity depths of 50, 100 and 150  $\mu\text{m}$ . Then, TiO<sub>2</sub> was sputtered with thicknesses: 270, 650 and 1000 nm; named T1, T2 and T3. For all the 3D photocatalysts, a continuous and compact layer was observed. SEM cross-sectional images in **Figure 1c-d** show the characteristic columnar growth of TiO<sub>2</sub> deposited by sputtering.

The GI-XRD pattern of TiO<sub>2</sub> (**Figure 2a**) shows the characteristic peaks of anatase at  $2\theta = 25.24^\circ$  for the (101) plane and of rutile at  $2\theta = 27.39^\circ$  for the (110) plane<sup>9</sup>, with the composition of each phase being 77.15% and 22.85%, respectively. The absorption spectra of the TiO<sub>2</sub> (**Figure 2b**) confirms the strong absorption of TiO<sub>2</sub> in the UV range from 200 to 349 nm. XPS Ti 2p (**Figures 2c**) spectrum exhibits the characteristic spin-orbit splitting peaks that show the contribution of the Ti<sup>4+</sup> and Ti<sup>3+</sup> components. And, O 1s spectra showed the component at 530.3 eV ascribed to the O<sup>2-</sup> bound to Ti<sup>4+</sup>. XPS Ti 2p (and O 1s spectra have the stoichiometric signature corresponding to TiO<sub>2</sub>.<sup>10</sup>

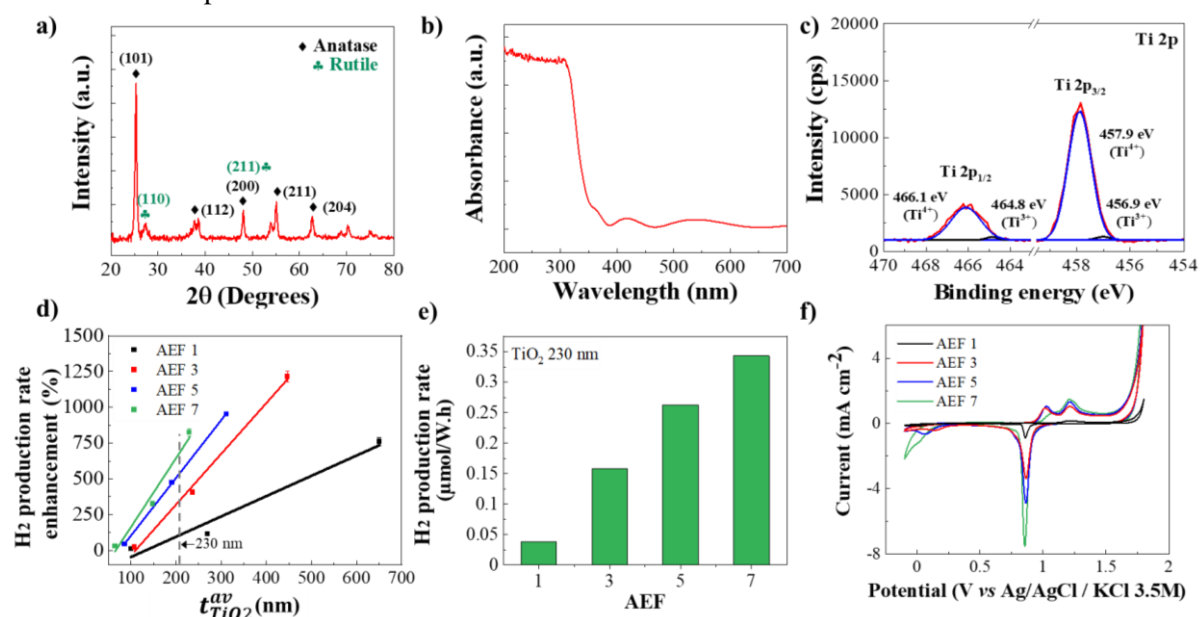


**Figure 2.** Characterization of TiO<sub>2</sub> 270 nm film: (a) GI-XRD pattern, (b) UV-Vis absorption spectra and (c) Ti 2p<sub>1/2,3/2</sub> XPS spectrum. H<sub>2</sub> production rate of 3D photocatalyst: (d) Enhancement as a function of the TiO<sub>2</sub> thickness and (d) Impact of AEF on H<sub>2</sub> production rate. (d) Cyclic voltammograms of 3D photocatalyst with T3.

Regarding the 3D photocatalyst film thickness, it was noted that it is not conformal along the depth microcavities. The thickness on the horizontal surfaces decreases from the top to bottom of the microcavities by a factor of 2.4, 4.0 and 9.9 for AEF values of 3, 5 and 7. To quantify the impact of this fluctuation, an average film thickness  $t_{\text{TiO}_2}^{\text{av}}$  was defined for each photocatalyst. **Figure 2d** shows that the surface area enlargement clearly boosts the photocatalytic activity, which leads to a remarkable enhancement of the H<sub>2</sub> production rate of 1214% compared to the planar topology. Yet not only the AEF impacts the H<sub>2</sub> production rate but also the TiO<sub>2</sub> layer thickness. The photocatalyst with an AEF = 3 exhibits a higher photocatalytic performance; this behavior can be ascribed to the semiconductor layer uniformity. This remarkable enhancement of a 3D photocatalyst with respect to a planar topology surpassed the expected results, where the efficiency was expected to be directly proportional to the surface area.

This establishes that higher efficiencies can be achieved by increasing the AEF when a nearly conformal TiO<sub>2</sub> layer with a minimum thickness of 200 to 300 nm is deposited. Based on this **Figure 2e** shows the predicted H<sub>2</sub> production rate for a conformal TiO<sub>2</sub> layer. The H<sub>2</sub> enhancement is by factors of 4, 7 and 9 for AEF values of 3, 5 and 7. This indicates that when microstructures with a higher aspect ratio  $\geq 1.4$  and a conformal TiO<sub>2</sub> layer are deposited and H<sub>2</sub> production linearly follows surface augmentation.

To corroborate the theoretical AEF, cyclic voltammetry experiments were carried out for 3D photocatalysts which exhibited the best H<sub>2</sub> production rate. The AEF was calculated by the integration of the reduction peak of Au in the cyclic voltammograms (**Figure 2f**).<sup>11</sup> AEF results for the theoretical AEF 3, 5 and 7 were  $6.53 \pm 0.06$ ,  $7.57 \pm 0.04$  and  $9.59 \pm 0.03$ , respectively. As seen, the experimental values are higher than the theoretical; yet, they reflect the same increasing trend which not only proves the change in depth of the microcavities, but it also considers the roughness and fluctuations associated to the polycrystalline surface of TiO<sub>2</sub>.

## IV. CONCLUSIONS

The photocatalytic performance for the H<sub>2</sub> production of 3D photocatalysts composed of TiO<sub>2</sub> and TiO<sub>2</sub>/Au NPs was reported as a function of semiconductor layer thickness and the aspect ratio relative to specific AEF values. We have demonstrated that, by augmenting the surface area by a factor of 3, H<sub>2</sub> production is enhanced by a factor of 12, due to the increase in active surface area for the water-splitting reaction.

## V. REFERENCES

- <sup>1</sup> L. Barreto, A. Makihira, and K. Riahi, *International Journal of Hydrogen Energy* **28**, 267 (2003).
- <sup>2</sup> H. Dotan, A. Landman, S.W. Sheehan, K.D. Malviya, G.E. Shter, D.A. Grave, Z. Arzi, N. Yehudai, M. Halabi, N. Gal, N. Hadari, C. Cohen, A. Rothschild, and G.S. Grader, *Nat Energy* **4**, 786 (2019).
- <sup>3</sup> N. Fajrina and M. Tahir, *International Journal of Hydrogen Energy* **44**, 540 (2019).
- <sup>4</sup> E. Eustache, P. Tilmant, L. Morgenroth, P. Roussel, G. Patriarche, D. Troadec, N. Rolland, T. Brousse, and C. Lethien, *Adv. Energy Mater.* **4**, 1301612 (2014).
- <sup>5</sup> J. Wang, H. Shao, S. Ren, A. Hu, and M. Li, *Applied Surface Science* **539**, 148045 (2021).
- <sup>6</sup> J. Cure, H. Assi, K. Cocq, L. Marin, K. Fajerweg, P. Fau, E. Bêche, Y.J. Chabal, A. Estève, and C. Rossi, *Langmuir* **34**, 1932 (2018).
- <sup>7</sup> M.-I. Mendoza-Diaz, J. Cure, M.D. Rouhani, K. Tan, S.-G. Patnaik, D. Pech, M. Quevedo-Lopez, T. Hungria, C. Rossi, and A. Estève, *J. Phys. Chem. C* **124**, 25421 (2020).
- <sup>8</sup> J. Cure, K. Cocq, A. Nicollet, K. Tan, T. Hungria, S. Assie-Souleille, S. Vivies, L. Salvagnac, M. Quevedo-Lopez, V. Maraval, R. Chauvin, A. Estève, and C. Rossi, *Adv. Sustainable Syst.* **4**, 2000121 (2020).
- <sup>9</sup> O. Secundino-Sánchez, J. Diaz-Reyes, J.F. Sánchez-Ramírez, and A.J.L. Jiménez-Pérez, *Rev. Mex. Fís.* **65**, 459 (2019).
- <sup>10</sup> E. Silva Junior, F.A. La Porta, M.S. Liu, J. Andrés, J.A. Varela, and E. Longo, *Dalton Trans.* **44**, 3159 (2015).
- <sup>11</sup> M. Łukaszewski, Soszko, M, and Czerwiński, A, *Int. J. Electrochem. Sci.* 4442 (2016).